Plant Physiology and Biochemistry 216 (2024) 109123

Contents lists available at ScienceDirect

Plant Physiology and Biochemistry

journal homepage: www.elsevier.com/locate/plaphy

The role of the *Arabidopsis* tandem zinc-finger C3H15 protein in metal homeostasis

Amparo Andrés-Bordería [a], Laia Mazuque-Pons [b], Marta Romeu-Perales [b], Antoni Garcia-Molina [b,1], Nuria Andrés-Colás [b,2], María Teresa Martínez-Pastor [a,b], Amparo Sanz [c], Sergi Puig [a], Lola Peñarrubia [b], Ana Perea-García [b,*]

[a] Departamento de Biotecnología, Instituto de Agroquímica y Tecnología de Alimentos (IATA), Consejo Superior de Investigaciones Científicas (CSIC), Paterna, Valencia, Spain
[b] Departament de Bioquímica i Biologia Molecular, Universitat de València, Burjassot, Valencia, Spain
[c] Departament de Biologia Vegetal, Universitat de València, Burjassot, Valencia, Spain

ARTICLE INFO

Handling Editor: Dr K Kees Venema

Keywords:
Arabidopsis thaliana
ARE
C3H14
C3H15
Copper
Post-transcriptional regulation
Zinc

ABSTRACT

Living organisms have developed finely regulated homeostatic networks to mitigate the effects of environmental fluctuations in transition metal micronutrients, including iron, zinc, and copper. In *Saccharomyces cerevisiae*, the tandem zinc-finger protein Cth2 post-transcriptionally regulates gene expression under conditions of iron deficiency by controlling the levels of mRNAs that code for non-essential ferroproteins. The molecular mechanism involves Cth2 binding to AU-rich elements present in the 3′ untranslated region of target mRNAs, negatively affecting their stability and translation. *Arabidopsis thaliana* has two TZF proteins homologous to yeast Cth2, C3H14 and C3H15, which participate in cell wall remodelling. The present work examines the expression of representative metal homeostasis genes with putative AREs in plants with altered levels of C3H14 and C3H15 grown under varying metal availabilities. The results suggest that C3H15 may act as a post-transcriptional plant modulator of metal adequacy, as evidenced by the expression of *SPL7*, the main transcriptional regulator under copper deficiency, and *PETE2*, which encodes plastocyanin. In contrast to *S. cerevisiae*, the plant C3H15 affects copper and zinc homeostasis rather than iron. When grown under copper-deficient conditions, adult $C3H15^{OE}$ plants exhibit lower chlorophyll content and photosynthetic efficiency compared to control plants, suggesting accelerated senescence. Likewise, metal content in $C3H15^{OE}$ plants under copper deficiency shows altered mobilization of copper and zinc to seeds. These data suggest that the C3H15 protein plays a role in modulating both cell wall remodelling and metal homeostasis. The interaction between these processes may be the cause of altered metal translocation.

1. Introduction

In eukaryotes, zinc-finger (ZF) are the most common motifs in metallo-regulatory proteins, mediating DNA binding of transcription factors, RNA binding of post-transcriptional modulators, and protein-protein interactions. The zinc-binding motifs are constituted of cysteine (C) and histidine (H) residues with specific arrangements that confer the ability to interact with nucleic acids. A subgroup of the ZF protein superfamily are the tandem zinc-finger (TZF) proteins, which function as regulatory factors, mainly at the post-transcriptional level, and are conserved from yeast to metazoans. At the molecular level, TZF proteins bind to the 3′-UTRs region of mRNAs that contain AU-rich elements (AREs), and limit their expression by promoting mRNA decay and/or inhibiting translation (Lai et al., 2014). In both yeast and mammals, TZF proteins such as Cth2 and tristetraprolin (TTP), respectively, are expressed in response to iron (Fe) deficiency. This promotes the post-transcriptional down-regulation of ARE-containing mRNAs that encode proteins that participate in Fe-dependent metabolic pathways, in order to optimize metal utilisation (Puig et al., 2005; Ahn and Jun 2007).

* Corresponding author.
E-mail address: ana.perea@uv.es (A. Perea-García).
[1] Centre for Research in Agricultural Genomics, Spanish National Research Council (CSIC), Barcelona, Spain.
[2] Instituto de Biología Molecular y Celular de Plantas, Universitat Politècnica de València-Consejo Superior de Investigaciones Científicas (CSIC), Valencia, Spain.

https://doi.org/10.1016/j.plaphy.2024.109123
Received 5 June 2024; Received in revised form 26 August 2024; Accepted 10 September 2024
Available online 11 September 2024

A. thaliana possesses 68 genes that encode proteins containing TZFs, which are characterised by the presence of three cysteine residues and a single histidine, denoted CCCH (Wang et al., 2008). Most of them exhibit a divergent pattern from the TZF spacing consensus, and are preceded by arginine-rich (RR) domains. CCCH TZFs typically are composed by 1–6 copies of CCCH motifs (Bogamuwa and Jang, 2014; Jang, 2016). Depending on the number and the C/H spacing pattern, plant CCCH TZFs are classified into 11 different subfamilies with different expression patterns and functions (Pomeranz et al., 2010). Plant TZF proteins are involved in a wide variety of developmental and adaptive processes, including seed germination, embryo formation, floral reproductive organ identity, determination of plant and floral reproductive organ architecture, leaf senescence, and abiotic stress responses (Li and Thomas, 1998; Sun et al., 2007; Xie et al., 2019; Yamasaki et al., 2007, 2009; Zhang et al., 2012). Two *Arabidopsis* proteins from subfamily II, C3H14 and C3H15, contain $Cx_8Cx_5Cx_3H$ motifs, as described for ScCth2. The C3H14 protein exerts a relevant role in the formation of the secondary wall by activating the expression of biosynthetic genes related in this process (Kim et al., 2012). Both C3H14 and its homologue C3H15 exhibit functions involved in the regulation of secondary wall thickening, as well as in anther development and pollen formation. This regulation occurs at both the transcriptional and post-transcriptional levels. Several gene expression analyses, conducted using microarrays and RT-qPCR show that C3H14 and C3H15 negatively regulate the expression of genes involved in the thickening of the secondary cell wall, including *IRX15* and *GXM1*, or the multicopper oxidase *LAC17* (Chai et al., 2015). In addition to the high Cu quota represented by cell wall multicopper oxidases, cell wall composition and thickness play an important role in metal chelation and mobilisation. This is due to the presence of negative charges that interact, among other particles, with the divalent cations causing their retention (Curie and Mari, 2017). Moreover, cell-to-cell signalling via plasmodesmata is modified by metal availability through callose deposition (O'Lexy et al., 2018).

The mechanism that controls the acquisition of specific metals involves a general metal sensor that detects the metal content within the cell. Consequently, it regulates the machinery for the acquisition, distribution, and delivery of appropriate amounts of metal throughout the cells. In *A. thaliana*, SPL7 (SQUAMOSA PROMOTER-BINDING PROTEIN-LIKE 7) is the main transcriptional regulator in the response to Cu deficiency. It functions by binding to consensus GTAC sequences, located at the target promoters of Cu deficiency-responsive genes (Nagae et al., 2008; Yamasaki et al., 2009). The fact that *SPL7* transcript levels remain largely constant at different Cu statuses suggests its post-transcriptional regulation (Bernal et al., 2012; Yamasaki et al., 2009). Among the SPL7 targets are high-affinity copper transporter (COPT) genes, and several microRNAs, denoted as Cu-miRNA. These microRNAs have been demonstrated to degrade transcripts encoding non-essential cuproproteins, thereby directing the scarce Cu present to essential cuproproteins such as chloroplastic plastocyanin (PC) (Burkhead et al., 2009; Pilon et al., 2009; Yamasaki et al., 2007). The molecular bases of subcellular metal distribution driving metals towards organelles such as mitochondria and chloroplasts remain unknown despite their importance. Since at the molecular level, these putative modulators are mainly miRNAs and mRNA-binding proteins, such as TZF proteins (Perea-García et al., 2022), to check if homologues of modulators described in other organisms could also play this function in plants.

Whereas the *S. cerevisiae* Cth2 protein and its human homologue TTP act as post-transcriptional modulators of mRNAs encoding iron-containing or iron metabolism-related proteins under Fe deficiency, the *Arabidopsis* homologue C3H15 has been reported to participate in cell wall remodelling and callose metabolism during microsporogenesis (Chai et al., 2015; Lu et al., 2014). In this sense, the present work studies whether C3H15 function is also related to metal homeostasis and to ascertain how this putative new role with can be reconciled with the previously established function in cell wall modification and plasmodesmata permeability. Additionally, we explore whether the role of C3H15 in these processes affects whole plant metal distribution when metal availability is inadequate.

2. Materials and methods

2.1. Plant material and growth conditions

Seeds of the Wild-Type (WT), $COPT1^{OE}$, $COPT3^{OE}$, $C3H14^{OE}$, $C3H15^{OE}$ and *c3h14c3h15(±)* genotypes of *A. thaliana* cv Columbia 0, were grown during 7 d on plates as previously described (Andrés-Colás et al., 2013). The range of Cu-related variations involve: Cu deficiency (Cu not added), Cu sufficiency (1 μM $CuSO_4$), Cu excess (10 μM $CuSO_4$) and Cu severe excess (25 μM $CuSO_4$). In the case of Fe: Fe severe deficiency (Fe not added), Fe deficiency (10 μM Fe-citrate), Fe low deficiency (25 μM Fe-citrate), Fe sufficiency (50 μM Fe-citrate) and Fe excess (100 μM Fe-citrate). Zn-related variation consists of: Zn severe deficiency (Zn not added), Zn sufficiency (15 μM $ZnSO_4$) and Zn excess (75 and 150 μM $ZnSO_4$).

For hydroponic cultures, seeds of the WT, $C3H14^{OE}$, $C3H15^{OE}$ and *c3h14c3h15(±)* genotypes were sown in 0.2 mL de-tipped eppendorfs containing MS media buffered with MES-KOH at pH 5.7, and 0.75 % (w/v) agar. To obtain synchronized germination the eppendorfs were suspended on a grid inside a container with distilled water and stratified for 2 d at 4 °C. Then they were transferred to a growth chamber, under a photo- and thermoperiod regime of 12 h light/23 °C and 12 h darkness/16 °C, 65–70 % relative humidity. After 8 d, the growing seedlings were transferred in their eppendorfs to Araponics trays (https://www.araponics.com/), containing 2 L of half-strength Hoagland nutrient medium for 8 d, and full-strength medium thereafter. The nutrient solution was prepared as described by Hermans and Verbruggen (2005) with small modifications: 10 mM $Ca(NO_3)_2$, 1 mM $MgSO_4$, 0.88 mM K_2SO_4, 0.25 mM KH_2PO_4, 50 μM FeEDDHA (Ferriete), 10 μM NaCl, 10 μM H_3BO_3, 1 μM $ZnSO_4$, 1 μM $MnSO_4$, 1 μM $CuSO_4$, and 0.01 μM $(NH_4)_6Mo_7O_2$. The solution was buffered with MES (0.05 g L^{-1}) and the pH adjusted to 5.7–5.8 with KOH. Treatments started when plants were 24-day-old. Sufficiency conditions (control medium) contained the indicated nutrients, while Cu, Zn and Fe deficiencies (-Cu, –Zn and -Fe media) were prepared without the addition of these micronutrients. The nutrient media were renewed weekly throughout the culture.

2.2. Plant growth measurements

For these experiments, 7–9 plants per genotype and nutrient medium were used in four independent replicates. Plant growth was followed as changes in plant weight and leaf area. Due to leaf overlapping within and between plants (F ig. S5) occurring from the 2nd week of treatment, foliar cover was determined instead of total area of leaves. For this purpose, zenithal pictures of the plants in the Araponic Hydroponic System of three of the replicates were taken at weekly intervals. Foliar cover was quantified from these pictures, using the automatic batch plugin of the program Easy Leaf Area (Easlon and Bloom, 2014) until the 3rd week from the onset of the treatments, and by manually selecting the plants' perimeter, avoiding empty gaps between leaves, with the ImageJ software (http://imagej.nih.gov/ij) in the 4th week after treatment.

Four weeks after the onset of the treatments the plants of two of the replicates were sampled and separated into roots, adult and developing rosette leaves and floral stems. To eliminate traces of nutrient medium from the apoplast, the roots were immersed in 2 μM EDTA for 30 s and then rinsed on a plastic sieve with running Milli-Q water. After blotting the roots with paper towel, the fresh weight (FW) of the plant organs was determined, and subsequently kept in a drying oven (Memmert UL 50) at 80 °C until constant weight (dry weight, DW).

2.3. Metal contents

The dry organs were ground to a fine powder with a porcelain or glass mortar and pestle to avoid any contact with metallic labware. The seeds obtained from hydroponic cultures were dried directly in a microwave oven. The seeds and three aliquot samples from one of the replicates were digested with trace metal grade HNO_3 and analyzed by ICP-MS (Agilent, mod. 7900) in the Servei Central de Suport a la Investigació Experimental (SCSIE) of the University of Valencia. Relative metals distribution in plant organs were calculated as metal concentration in shoots/metal concentration in roots.

2.4. Chlorophyll content and fluorescence

Chlorophyll content was measured after four weeks of treatment in adult leaves, using a chlorophyll meter (SPAD-502plus, Konika-Minolta). Results are given in relative units (SPAD units). The same leaves used for chlorophyll measurements were dark-adapted with *ad-hoc* clips for 30 min before determining the maximum quantum efficiency of photosystem II state (Fv/Fm) with a portable fluorometer (Os-30p+, OptiScience). Two independent replicates were used for these measurements. In each replicate three samples of three plants per genotype and nutrient medium were analyzed. An additional replicate was used to follow time-course changes along treatments.

2.5. Seed yield

To test possible differences in plant productivity due to genotype and/or nutritional conditions, floral stems of plants from one of the replicates were enclosed in paper bags until the siliques were fully mature and dry. Seeds were then collected and weighed. Three samples of three plants per genotype and nutrient medium were measured.

2.6. Protoplasts isolation and subcellular localization in Arabidopsis

Arabidopsis protoplasts were isolated from the fresh leaf tissue of the 3-week-old plants grown on soil, and were transformed as previously described (Abdel-Ghany et al., 2005). The complete *C3H15* coding sequence was obtained from *Arabidopsis* genomic DNA by regular PCR using specific primers (detailed in Supplementary Table SIII), which introduce the adequate restriction sites for cloning. The C-terminus was fused with the GFP reporter and its expression was controlled by the constitutive *CaMV35S* promoter through its insertion into the transient expression vector pGFPau with the *Spe*I and *Nco*I restriction enzymes. The *C3H15-GFP* construct was used to transform the *Arabidopsis* protoplasts. After 16 h under continuous light at 23 °C in the wash solution, confocal images were obtained using a fluorescence confocal microscope TCS SP vertical (DM-R) (Leica) equipped with an argon ion (458 and 488 nm), He-Ne I (543 nm) and He-Ne II (633 nm) excitation laser systems and a 60× objective lens. The fluorescence signals were detected at 500–530 nm for GFP and at 650–750 nm for chlorophyll, after exciting at 488 and 633 nm, respectively.

2.7. Gene expression by reverse-transcription quantitative PCR

Total *Arabidopsis* RNA was isolated using the Spectrum Plant Total RNA Kit (Sigma-Aldrich) and quantified by UV spectrophotometry and its integrity was visually assessed on ethidium bromide-stained agarose gels. After treatment with DNase I Recombinant, RNAse-free (Roche), cDNA was generated by retro-transcriptase Maxima Reverse Transcriptase (Thermo Scientific) as previously described (Sanvisens et al., 2014). Reverse-transcription quantitative PCR (RT-qPCR) was carried out with TB Green Premix® Ex Taq ™ (Tli RNaseH Plus) with ROX (Takara), with the specific primers detailed in Supplementary Table SIII, in a CFX96 Touch™ Real Time PCR Detection System (BioRad, Hercules, CA, USA), with one cycle of 95 °C for 2 min and 40 cycles consisting of 95 °C for 30 s and 60 °C for 30 s. Expression values were normalized to *UBQ10* and *ACTIN2* genes, using the 2^{-ddCt} method.

2.8. Three-hybrid assay

DNA fragments downstream stop codon containing putative AREs were obtained by PCR using the corresponding oligonucleotides (Table SIII). DNA fragments were sequenced, digested with the enzyme *Sma*I, and cloned into pIIIA-MS2.1 vector. To clone C3H15 protein, two fragments were used as a template, one with the sequence of the wild-type protein and another with a mutation in the TZF that prevents binding to RNA (C3H15-C243R). They were amplified using the corresponding oligonucleotides (Table SIII), digested with *BamH*I and *Xho*I enzymes, and cloned into the *pACT2* vector. Once both constructions were obtained, yeast strain L40 coat (from Dr. Marvin Wickens) was co-transformed. Yeast transformants were cultivated in SC-ura -leu to exponential growth phase, and then spotted at OD_{600} of 0.1 on SC-leu-ura, and SC-ura-leu-his (-His) plates with increasing concentrations of 3-aminotriazol (3-AT). All assays were performed in duplicate with two independent colonies. The cells were allowed to grow for 3 d at 30 °C.

2.9. Statistical analyses

The IBM-SPSS Statistics package (v 28.0) was used to establish statistically significant differences among means, either by one-way ANOVA and subsequent Tukey's tests or by t-tests. On the other hand, for the analysis of gene expression, a comparison of relative gene expression (RT-qPCR) was performed (p-value <0.05) (Pfaffl et al., 2002). For the remaining parameters in seedlings, the analyses were carried out using two-way ANOVA with the means compared by the Duncan's or Kruskal Wallis' test (p-value <0.05) using the InfoStat software, version 2008 (http://www.infostat.com.ar). Further details are given in Figure legends.

3. Results

3.1. Conservation of $Cx_8Cx_5Cx_3H$-containing proteins in yeast and plants

The yeast *S. cerevisiae* expresses two $Cx_8Cx_5Cx_3H$ proteins, Cth1 and Cth2, implicated in modulating Fe deficiency response (Puig et al., 2008). Two *Arabidopsis* TZF proteins from the CCCH subgroup II, AtC3H14 and AtC3H15, are the closest homologues to the yeast counterparts. Moreover, homologues are also present in other higher plants, including *Zea mays* (ZmC3H14 and ZmC3H15) and *Oryza sativa* (OsC3H14 and OsC3H15). A general overview of the plant sequences compared to yeast Cth1 and Cth2 indicates that there are specific regions where the homology is high, such as the TZF domain (F ig. S1). A comparison of the two CCCH motifs (1 and 2) indicates that CCCH1 is more conserved in higher plants than CCCH2 motif (Fig. 1A and B). Hence, the overlap of the two TZF motifs from Cth2 and AtC3H15 provides further evidence that the CCCH1 is the most conserved (Fig. 1C).

3.2. ARE presence in the Arabidopsis genome

In previous studies, the function of Arabidopsis C3H14 and C3H15 has been related to the formation and remodelling of cell walls, as well as callose metabolism during microsporogenesis (Lu et al., 2014; Chai et al., 2015). However, whether C3H14 and C3H15 have any relationship with metal homeostasis remains unexplored. Putative targets of C3H14 and C3H15 have been previously suggested in Arabidopsis through a comparative analysis of microarrays obtained from plants with altered levels of *C3H15* expression under standard metal conditions (Chai et al., 2015). However, the presence of AREs in the 3′-UTR of the genes that could be targets of C3H15 in Arabidopsis has not been studied. To analyze the presence of these sequences, an *in silico* study

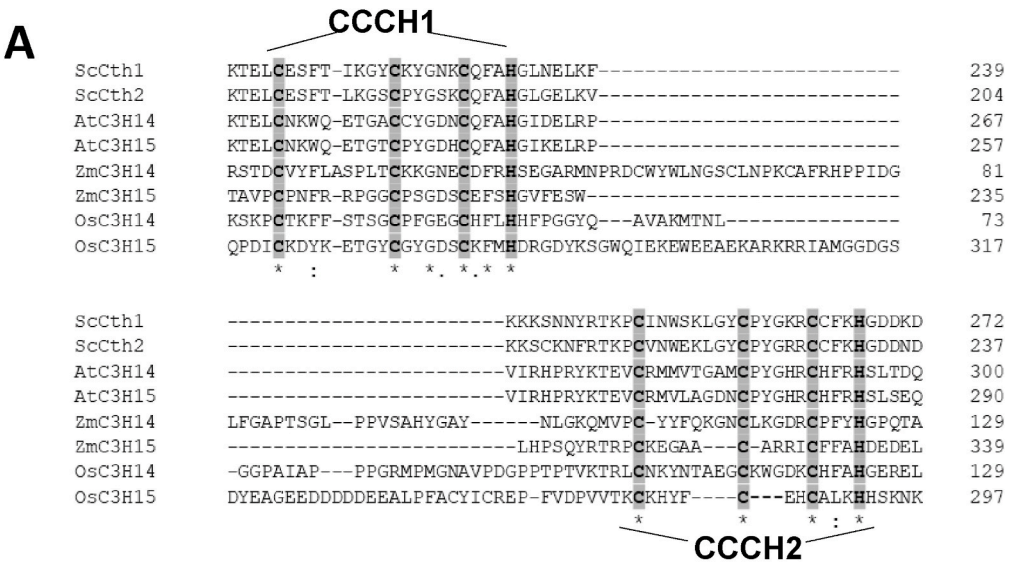

B

CCCH2

CCCH1	1	2	3	4	5	6	7	8
1.ScCth1		86.21	34.48	34.48	37.04	36.00	27.59	18.75
2.ScCth2	**82.76**		34.48	34.48	37.04	40.00	27.59	18.75
3.AtC3H14	**58.62**	**58.62**		75.86	25.93	32.00	34.48	12.50
4.AtC3H15	**58.62**	**62.07**	**86.21**		29.63	32.00	34.48	12.50
5.ZmC3h14	**28.57**	**25.00**	**21.43**	**25.00**		24.00	33.33	23.53
6.ZmC3H15	**34.48**	**37.93**	**34.48**	**37.93**	**25.00**		44.00	20.00
7.OsC3H14	**27.59**	**31.03**	**31.03**	**34.48**	**28.57**	**34.48**		18.75
8.OsC3H15	**31.03**	**31.03**	**37.93**	**37.93**	**25.00**	**31.03**	**24.14**	

C

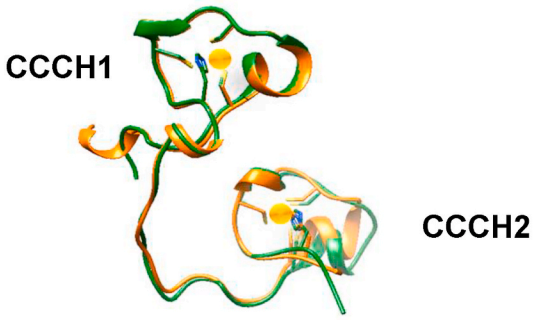

Fig. 1. TZF domain (TZF1 and TZF2) alignment of ScCth1 and ScCth2 from yeast and higher plants orthologs. A) Alignment of the Cth-like TZF domains from yeast and plants. The alignment was built using the Clustal Omega software and refined manually. Protein sequences from the UniProt Database (UniProt.org/) included: *Saccharomyces cerevisiae* ScCth1 (1) and ScCth2 (2), *Arabidopsis thaliana* AtC3H14 (3) and AtC3H15 (4), and *Zea mays* ZmC3H14 (5) and ZmC3H15 (6) *Oryza sativa* OsC3H14 (7) and OsC3H15 (8). The numbers shown at the right of each sequence are numbers of amino acid residues in the corresponding proteins. Gaps (marked with dashes) were introduced to maximize the sequence alignment. Conserved Cysteine (C) and Histidine (H) residues in the zinc fingers are in bold and gray shaded. An "*" (asterisk) at the bottom of the alignment indicates identical residues, a ":" (double colon) conserved substitutions and a "." (colon) semi-conserved substitutions. B) Percentage identity calculated using the alignments of TZF1 (bold numbers) and TZF2 (plain numbers). C) Overlapping of the TZF domains. The sequences from ScCth2 (orange) and AtC3H15 (green) shown in A) were overlapped with the program UCSF Chimera. Cys and His residues are indicated and the Zn atom shown in purple. Protein sequences from the UniProt Database (UniProt.org/) included: *Saccharomyces cerevisiae* ScCth1 (P47976) and ScCth2 (P47977), *Arabidopsis thaliana* AtC3H14 (Q9C9N3) and AtC3H15 (Q9C9F5), *Zea mays* ZmC3H14 (AOA060D4X8) and ZmC3H15 (AOA060D812) and *Oryza sativa* OsC3H14 (Q7F8R0) and OsC3H15 (Q6K4V3).

was conducted on the *A. thaliana* genes containing the canonical ARE *UUAUUUAUU* or one of the *UAUUUAUU* or *UUAUUUAU* variants, which could participate in the putative RNA-binding capacity of C3H14 and C3H15. In order to perform a complete study, the search was made within the 3′-UTR (when determined) and/or +1000 nt after the stop codon of the TAIR database (www.arabidopsis.org). This approach yielded 2268 genes containing the complete *UUAUUUAUU* sequence, 4510 genes containing the *UAUUUAUU* sequence, and 4713 genes with the *UUAUUUAU* sequence. After eliminating repeated genes, the final count was 6563 genes containing a putative ARE downstream of their stop codon. Once the list of genes was obtained, we found 103 genes related to Fe homeostasis that contain AREs (Table SI), 268 genes related to Zn with putative 3′-UTR ARE motifs (Table SII), and 62 genes for Cu homeostasis genes with putative AREs (Table 1). Among them, we found

Table 1
Putative ARE sequences present in genes related to copper homeostasis. ARE sequences at the 3′UTR regions and/or +1000 nt after the stop codon in *Arabidopsis thaliana* genome were filtered by "Gene Ontology" in the Copper Binding category. The copper homeostasis related genes are indicated with the identification (ID), name, description and the number of the AREs motifs. Underlined numbers indicate ARE UUAUUUAUU location and numbers without underlined indicate other AREs locations (UAUUUAUU o UUAUUUAU). * indicates that the ARE sequence found is in the 3′UTR sequence determinated in TAIR10. Bold letters indicates genes analyzed by RT-qPCR.

Gene ID	Gen Name	Gene Description	Nº AREs	position
AT1G08500	*ENODL18*	early nodulin-like protein 18	2	*863-870/ 956-963*
AT1G10630	*ARFA1F*	ADP-ribosylation factor A1F	1	*384-392**
AT1G12520	***CCS***	**copper chaperone for SOD1**	**1**	*755–763*
AT1G20340	***PETE2***	**plastocyanin 2**	**1**	*539-546**
AT1G21860	*SKS7*	SKU5 similar 7	1	*942–949*
AT1G49240	*ACT8*	actin 8	1	*765-772**
AT1G53030	*COX17-2*	cytochrome C oxidase copper chaperone (COX17)	1	*140-147**
AT1G55560	*SKS14*	SKU5 similar 14	1	*538–545*
AT1G55570	*SKS12*	SKU5 similar 12	1	*17-24**
AT1G63440	***HMA5***	**heavy metal ATPase 5**	**1**	*540–547*
AT1G64640	*ENODL8*	early nodulin-like protein 8	2	*19-27*/ 81–89**
AT1G72330	*ALAAT2*	alanine aminotransferase 2	1	*232–239*
AT1G79440	*ALDH5F1*	aldehyde dehydrogenase 5F1	1	*178-185**
AT1G79530	*GAPCP-1*	glyceraldehyde-3-phosphate dehydrogenase of plastid 1	2	*660–668*
AT2G02850	***ARPN***	**plantacyanin**	**2**	*190-197*/ 339-346*
AT2G05990	*MOD1*	NAD(P)-binding Rossmann-fold superfamily protein	1	*769–776*
AT2G15770	–	cupredoxin superfamily protein	1	*372–380*
AT2G15780	–	cupredoxin superfamily protein	1	*768–775*
AT2G23630	*SKS16*	SKU5 similar 16	2	*391-398/ 920-927*
AT2G23990	*ENODL11*	early nodulin-like protein 11	1	*233–241*
AT2G26975	***COPT6***	**Ctr copper transporter family**	**1**	*592–600*
AT2G30860	*GSTF9*	glutathione S-transferase PHI 9	1	*607–614*
AT2G33210	*HSP60-2*	heat shock protein 60-2	1	*330–337*
AT2G36460	*FBA6*	aldolase superfamily protein	2	*436-443/ 735-742*
AT2G37920	*emb1513*	copper ion transmembrane transporter	1	*973–981*
AT3G08580	*AAC1*	ADP/ATP carrier 1	1	*251-258**
AT3G09220	*LAC7*	laccase 7	1	*355–362*
AT3G15020	*mMDH2*	lactate/malate dehydrogenase family protein	2	*656-663/ 684-692*
AT3G17820	*GLN1.3*	glutamine synthetase 1.3	1	*504–511*
AT3G23940	–	dehydratase family	1	*75-83**
AT3G27200	–	cupredoxin superfamily protein	1	*390–398*
AT3G43670	–	copper amine oxidase family protein	1	*135-142**
AT3G54660	*GR*	glutathione reductase	1	*793–800*
AT3G55440	*TPI*	triosephosphate isomerase	1	*931–939*
AT4G12270	–	copper amine oxidase family protein	2	*457-464/ 500-507*
AT4G13850	*GR-RBP2*	glycine-rich RNA-binding protein 2	1	*617–625*
AT4G15940	–	fumarylacetoacetate (FAA) hydrolase family	1	*10-17**
AT4G20260	*PCAP1*	plasma-membrane associated cation-binding protein 1	1	*194-202**
AT4G22010	*SKS4*	SKU5 similar 4	1	*409–416*
AT4G25240	*SKS1*	SKU5 similar 1	1	*60-67**
AT4G30590	*ENODL12*	early nodulin-like protein 12	1	*395–402*
AT4G31840	*ENODL15*	early nodulin-like protein 15	1	*21-28**
AT4G32490	*ENODL4*	early nodulin-like protein 4	2	*715–722*
AT4G32610	–	copper ion binding protein	1	*445–452*
AT5G01050	–	laccase/Diphenol oxidase family protein	2	*287-294/ 896-903*
AT5G07475	–	Cupredoxin superfamily protein	1	*70-77**
AT5G15350	*ENODL17*	early nodulin-like protein 17	1	*641–648*
AT5G18830	***SPL7***	**SQUAMOSA promoter binding protein-like 7**	**1**	*590–598*
AT5G21105	*MCO3*	plant L-ascorbate oxidase	1	*656–663*
AT5G37600	*GSR 1*	cytosolic glutamine synthetase	2	*168-175*/ 412-419*
AT5G50370	–	adenylate kinase family protein	1	*566–574*
ATCG00580	*psbE*	photosystem II reaction center protein E	1	*867–875*

genes from the Early NODulin-Like protein (*ENODL*) family and from the Pectinesterase-like protein (*SKS*) family. It is noteworthy that the transcriptional regulator SQUAMOSA Like Protein 7 (*SPL7*), a key factor in the response to Cu deficiency (Bernal et al., 2012; Yamasaki et al., 2009) is also found among these genes. In addition, the gene encoding high affinity Cu transporter *COPT6* (Garcia-Molina et al., 2013) and the Cu-transporting P-type ATPase *HMA5*, involved in root-to-shoot Cu translocation (Andrés-Colás et al., 2006) were obtained (Table 1). Moreover, additional genes encoding proteins involved in Cu homeostasis, including the Cu chaperone *COX17-2* involved in the transport of Cu to the mitochondrial cytochrome *c* oxidase (Balandin and Castresana, 2002), and the of superoxide dismutase (SOD) *CCS* (Abdel-Ghany et al., 2005). Curiously the genes encoding FeSOD (*FSD1*), which is a direct SPL7 target involved in SOD substitution under Cu deficiency (Abdel-Ghany and Pilon, 2008), and the gene encoding the most abundant plastocyanin isoform, *PETE2*, which has been proposed to function buffering Cu under Cu excess (Abdel-Ghany, 2009), also contain ARE motifs. Finally, the gene encoding basic blue Cu plantacyanin (*ARPN*), involved in the development of anthers (Dong et al., 2005), contains two putative ARE regulatory elements (Table 1). Taken together, genes related to copper regulation, mobilisation and redistribution have putative ARE elements, which could be involved in the putative RNA-binding capacity of C3H14 and C3H15.

3.3. Potential functional analogies between Cth2-like proteins

To ascertain whether C3H15 binds to mRNA containing AREs *in vivo*, a yeast three-hybrid assay was carried out (Fig. 2A). First, we tested whether the C3H15 protein binds to the ARE-containing mRNAs *SDH4* and *ACO1* from *S. cerevisiae*. The growth in SC-ura-leu-his (-His) medium revealed interactions between C3H15 protein and both-*ScSDH4* and *ScACO1* mRNAs, as observed for the Cth2 control (Fig. 2A). The interaction between C3H15 and the mRNA was lost in both cases when the cysteine residue at position 243 was mutated to arginine (C3H15-C243R). Moreover, the partial or complete mutation of the AREs present in *SDH4* mRNA (*ScSDH4-mt1* and *ScSDH4-mt2*, respectively, Puig et al., 2005) decreased or completely removed interaction (Fig. 2A). Taken together, these results demonstrate that the C3H15 protein has the ability to specifically bind *in vivo* to mRNAs with AREs in a manner that depends on the integrity of both its TZFs and the AREs within the target mRNA.

Next, the subcellular localization of C3H15 fused to the green fluorescence protein (GFP) (C3H15-GFP) was analyzed by transient expression under the control of the *CaMV35S* promoter in *Arabidopsis* protoplasts. The GFP signal obtained confirm a localization of C3H15 in specific cytosolic foci excluding the plasma membrane and chloroplasts (Fig. 2B). This punctuated C3H15 localization is consistent with a localization of C3H15 in stress granules (Chai et al., 2015, 2024; He

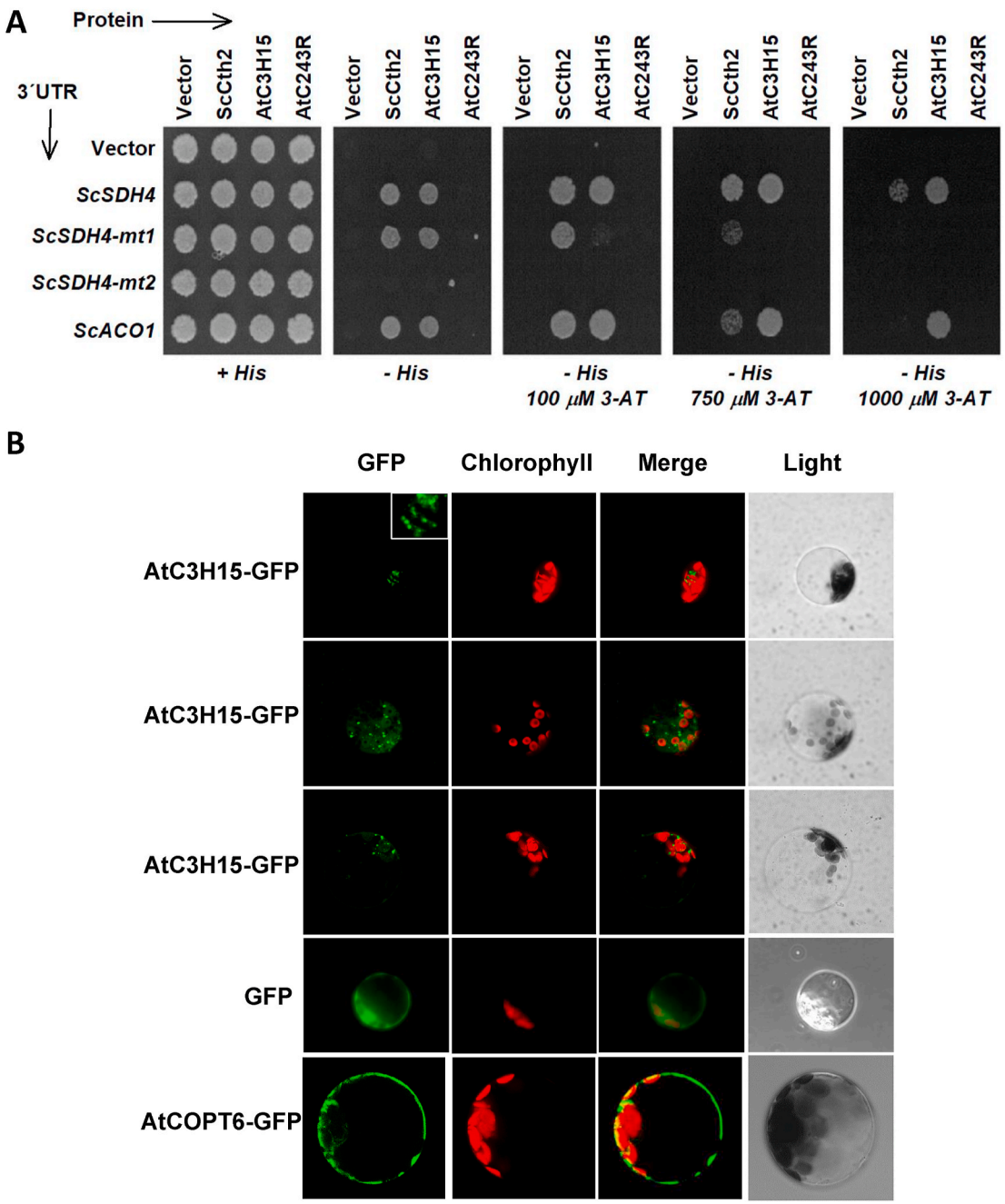

Fig. 2. *Arabidopsis* C3H15 protein specifically binds ARE-containing mRNAs. A) Yeast three hybrid protein-RNA interaction assay. Drop test assay with L40 coat strain co-transformed with different combinations of Cth2 protein-like (ScCth2, AtC3H15, and AtC3H15-C243R) and RNA (*SDH4* or *ARPN*), in SC-ura-leu + his (+His) and SC-ura-leu-his (-His) with different concentrations of the His3 inhibitor 3-aminotriazole (3-AT). Plates were incubated for 2 days at 30 °C and photographed. B) AtC3H15 subcellular localization by transient expression of AtC3H15-GFP construct in *Arabidopsis* protoplasts. GFP and AtCOPT6-GFP constructs were used as controls. Green and red fluorescence separated and overlapped, and the bright field image are shown.

et al., 2024).

3.4. Regulation of Arabidopsis C3H14 and C3H15 expression according to nutritional status

To ascertain whether the expression of *C3H14* and *C3H15* was regulated by different metal availability, *A. thaliana* seedlings were grown for 7 d in plates with MS medium on a scale from metal deficiency to excess of Fe, Zn and Cu. The RT-qPCR results obtained under these conditions show that neither *C3H14* nor *C3H15* transcript levels changed under Fe deficiency (Fi g. S2A), in contrast to what occurs in *S. cerevisiae* (Puig et al., 2005). Zn did not alter transcript levels of *C3H14*, whereas *C3H15* levels negatively correlated with Zn supply in the medium (F ig. S2B). However, Cu excess commonly induced *C3H14* and *C3H15* transcript levels in WT seedlings (Fig. 3A). Furthermore, in the case of *C3H15,* this increase was stronger in transgenic plants overexpressing high affinity Cu transporters such as COPT1 and COPT3, which enhance intracellular copper levels (Fi g. S3) (Andrés-Colás et al., 2010). Thus, these results suggest a putative regulatory role of C3H15 protein under Zn deficiency, and that of both C3H14 and C3H15 proteins in Cu excess.

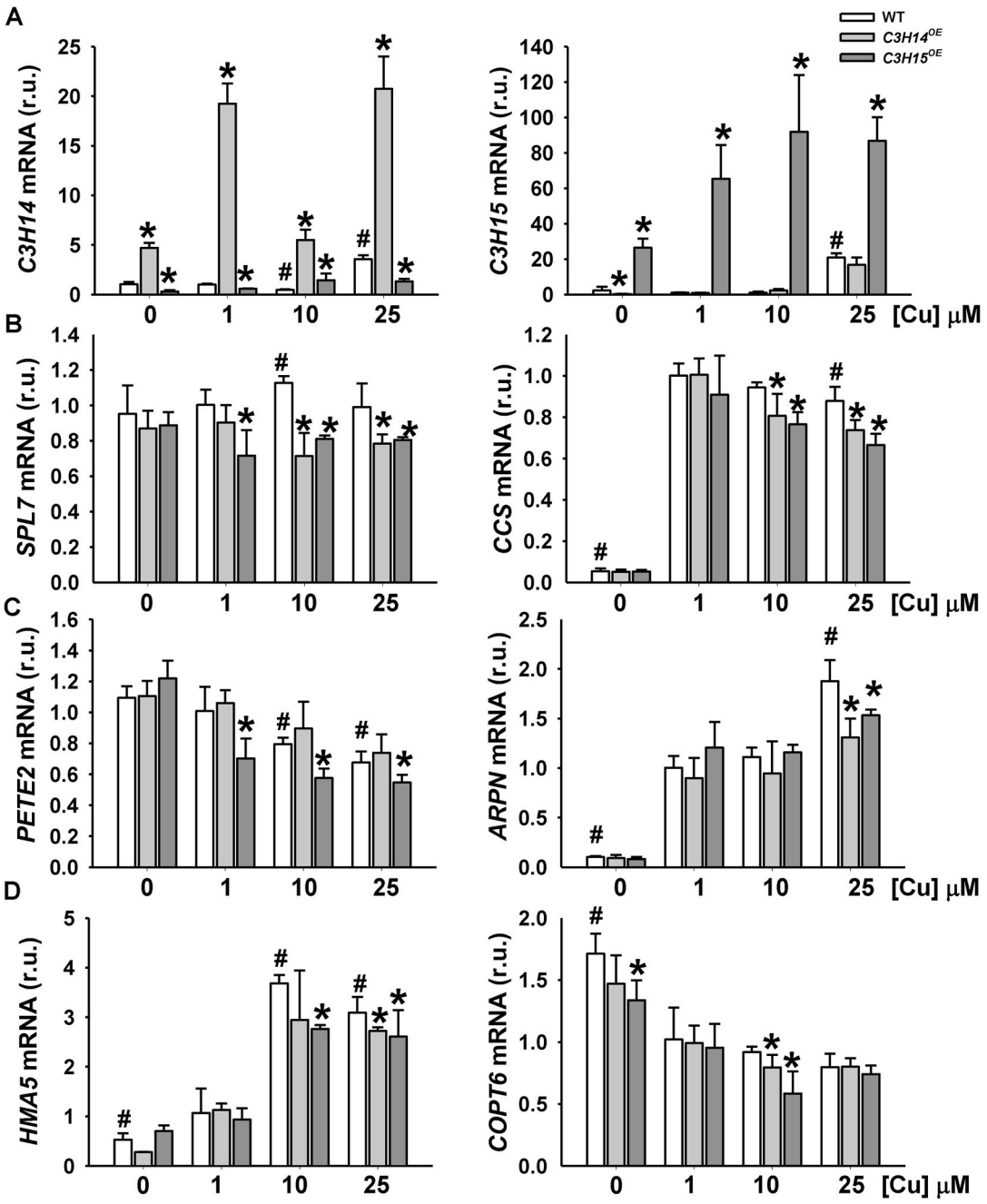

Fig. 3. Relative expression of metal homeostasis genes**.** The relative expression of the A) *C3H14, C3H15*, B) *SPL7*, *CCS*, C) *PETE2, ARPN*, D) *HMA5 and COPT6* genes were determined by RT-qPCR in 7-day-old WT, *C3H14*^{OE} and *C3H15*^{OE} seedlings, grown in different concentrations of Cu: deficiency (0 μM $CuSO_4$), sufficiency (1 μM $CuSO_4$), low excess (10 μM $CuSO_4$) and excess (25 μM $CuSO_4$) in the medium. The *ACTIN2* and *UBQ10* genes were used as references. mRNA levels are expressed as relative units (r.u.). The bars represent the mean ± SD of three replicates. * indicates significant differences between overexpressing plants against its WT in the same condition, # indicates significant differences of WT vs WT under sufficiency condition ($p < 0.05$).

3.5. Characterization of gene expression pattern in seedlings with altered C3H14 and C3H15 levels

In order to assess the putative regulatory effect of C3H14 and C3H15, 7-day-old seedlings ectopically expressing *C3H14* and *C3H15* under the *CaMV35S* promoter (*C3H14*^{OE} and *C3H15*^{OE}) (Chai et al., 2015) were grown on a Cu scale, ranging from deficiency (0 μM), sufficiency (1 μM) to mild (10 μM) and severe (25 μM) Cu excess (Fig. 3) (Andrés Colás et al., 2010). *C3H14* transcript levels were increased in *C3H14*^{OE} seedlings with respect to WT in each condition analyzed (Fig. 3A left panel) and the same is true for the *C3H15* levels in *C3H15*^{OE} seedlings (Fig. 3A right panel).

In order to corroborate the previously described targets for the C3H14 and C3H15 proteins under our experimental conditions, we first analyzed the expression of *LHCB2.3* (Light-Harvest Chlorophyll *a*/b-Binding protein 2.3) and *LAC17* (Laccase 17) genes obtained by Chai et al. (2015). In WT plants, the expression of these two genes decreases under both Cu deficiency and excess (F ig. S4A). Moreover, according to the role as post-transcriptional negative regulators of *C3H14* and *C3H15*, the expression of *LHCB2.3* and *LAC17* in *C3H14*^{OE} and *C3H15*^{OE} seedlings was reduced compared to the WT under sufficiency (Cu 1 μM), but this effect disappears under Cu deficiency and excess. Thus, the previously described C3H14 and C3H15-mediated negative modulation of gene expression is dependent on Cu availability.

The expression of several genes related to Cu, Fe and Zn homeostases that contain AREs (indicated in bold in Ta ble I, SI and SII), was also evaluated, including three important transcriptional regulators, *SPL7, bHLH121/URI* and *ZAT12* (Fig. 3 and S4). A consistent pattern of regulation was observed only in the case of Cu homeostasis genes (Fig. 3). Thus, *SPL7* expression remained mostly unaffected by the Cu status in WT seedlings. However, statistically significant differences in expression were found in the overexpressing seedlings under mild and severe Cu excess conditions when compared to their respective WT (Fig. 3B). A similar pattern was observed for the Cu chaperone for Cu/ZnSOD, CCS (Abdel-Ghany et al., 2005), which was found to be down-regulated in the overexpressing plants under high different Cu conditions (Fig. 3B). Moreover, other homeostatic Cu-related genes, such as *PETE2, ARPN, HMA5* and *COPT6* displayed lower levels depending on the specific overexpressing line and Cu conditions. Thus, while *PETE2* expression is only reduced in the *C3H15*^{OE} plants by Cu, *ARPN* and *HMA5* expression was reduced in both overexpressing lines under severe Cu excess and *COPT6* expression decreases in the overexpressing lines under mild Cu excess (Fig. 3C–D). This effect is reversed in the *c3h14c3h15(±)* mutant in some of the conditions tested (F ig. S5). The expression of *bHLH121*, an essential component of the Fe deficiency-signaling pathway (Kim et al., 2019), remains mostly unaffected in the overexpressing seedlings (F ig. S4B). On the other hand, the expression of the putative Fe vacuolar transporter *VTL2* is down-regulated under high Cu in the *C3H14*^{OE} and *C3H15*^{OE} seedlings (Fi g. S4B). Furthermore, in the case of Zn homeostasis, the expression of ZAT12, a zinc-finger protein involved in several abiotic stresses acclimation (Xie et al., 2019), increases under Cu excess in *C3H15*^{OE} plants (F ig. S4C). However, *ZNE1*, a Zn homeostatic component (Wang et al., 2021), is slightly up-regulated under low Cu in the *C3H145*^{OE} and *C3H15*^{OE} plants (F ig. S4C).

Taken together, these results indicate that among the three metals, the expression of Cu homeostasis genes with putative AREs (Table 1) is the most consistently affected, being reduced in the *C3H14*^{OE} and *C3H15*^{OE} seedlings under high Cu (Fig. 3). These results suggest a role for these TZFs as negative post-transcriptional regulators of ARE-containing Cu homeostasis genes under Cu excess.

3.6. Metal content of seedlings with altered C3H14 and C3H15 levels

Due to the interconnections between metal homeostatic networks (Perea-García et al., 2013; Waters et al., 2012), the total content of Cu, Fe and Zn was determined by ICP-MS in *C3H14*^{OE} and *C3H15*^{OE} seedlings grown as above. The aerial part and roots were separately collected, and the metal content and the relative distribution were calculated (Fig. 4). As expected, plant Cu content increases with Cu concentration in the growth medium in both shoots and roots. However, no significant differences were observed among the genotypes in the shoots except for a slight decrease in the overexpressing roots under high Cu content. This fact results in increased Cu relative distribution in *C3H15*^{OE} seedlings (Fig. 4A). On the other hand, the Fe content in the aerial part of WT seedlings decreases with increasing Cu concentration in the growing medium but increases in roots and not statistically significant differences were detected between in the overexpressing plants. These results indicate that the increasing Cu content in the medium decreases Fe relative distribution (Fig. 4B). With regard to Zn, the Zn content decreases in WT seedlings as Cu increases in the medium, both in the aerial part and in the roots under Cu excess with no significant relative distribution effects depending on Cu content. In comparison to the WT, the Zn content in *C3H15*^{OE} plants is higher in the aerial part and lower in the roots of the overexpressing plants under Cu deficiency, driving to an increased Zn relative distribution in overexpressing plants (Fig. 4C).

In addition, given that C3H15 is involved in the remodelling of the cell wall (Chai et al., 2015), and to ascertain whether this process affects the metal retaining capacity, the Cu, Fe and Zn content was determined in protoplasts from adult *Arabidopsis* plants. To this end, leaves from three genotypes were collected from leaves of 2- month-old *Arabidopsis* plants grown on soil conditions and the metal content was determined (Fig. 4). Although there was a slight reduction in the Cu content in the

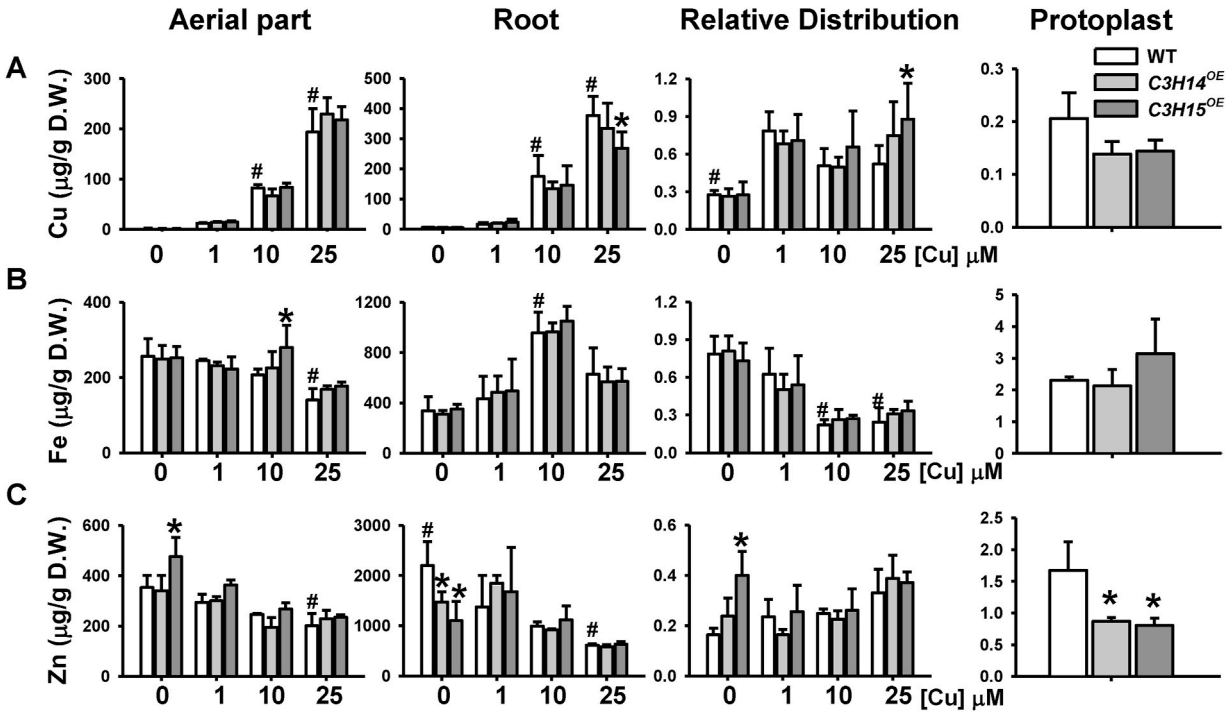

Fig. 4. Metal content in different tissue of seedlings by Cu status. A) Cu, B) Fe and C) Zn content of 7-day-old WT, *C3H14*^{OE} and *C3H15*^{OE} plants, grown in different external concentration of Cu; deficiency (0 μM $CuSO_4$), sufficiency (1 μM $CuSO_4$), low excess (10 μM $CuSO_4$) and excess (25 μM $CuSO_4$). Values correspond to aerial part, root, relative distribution (metal concentration in aerial part/metal concentration in root) and protoplasts. Statistical analysis was performed by two-way anova Duncan's test. * indicates significant differences between overexpressing plants against its WT in the same condition ($p < 0.05$).

protoplasts of the overexpressing plants compared to WT, this reduction was only statistically significant in the case of Zn (Fig. 4C).

3.7. Phenotypic characterization of plants with altered C3H15 levels grown under metal deficiency

Based on the metal content and relative distribution results in seedlings, and the metal content in leaf protoplasts from adult plants, we hypothesized that the consequences of the C3H14/C3H15 roles in cell wall remodelling and metal homeostasis could contribute to long-term phenotypic differences in metal distribution in plants. Moreover, the *C3H15* gene expression is higher in the vascular bundles of floral stems (Chai et al., 2015), further reinforcing that long distance transport of metals could be affected in *C3H15* overexpressing adult plants. To study these transport processes under controlled nutritional conditions, hydroponic cultures of WT and *C3H15*^{OE} plants were performed under several metal nutritional conditions of Cu, Zn and Fe both deficiencies and excess. Since no obvious phenotypes were observed except for Cu and Zn deficiencies, only these data were further analyzed. Thus, 24-day-old WT and *C3H15*^{OE} plants were grown under sufficiency (Control, Ctr), Cu deficiency (-Cu), Zn deficiency (-Zn) and Fe deficiency conditions for 4 weeks until floral stems were developed to study the effects on plant growth due to metal distribution defects.

The general aspects of the plants after treatments and separated rosette leaves are shown in F ig. S6. In general, *C3H15*^{OE} plants perform worse visually in any of the conditions, being these effects more drastic under Cu deficiency. During the four weeks of treatments, different morphological, physiological and biochemical parameters such as fresh and dry weights (F.W. and D.W.), water content, length, leaf area cover and chlorophyll content and fluorescence parameters were measured at different organs (young and old leaves, floral stems and roots), as well as seed yield (Fig. 5, S7, S8 and Table SIV). The pPlant growth, measured as changes in foliar cover, followed typical sigmoid curves (F ig. S7A), increasing similarly in both genotypes in the three media tested during the first two weeks of treatment. After the maximum absolute growth rate (AGR) was reached, growth decreased in both genotypes but to a lesser extent in WT than in the *C3H15*^{OE} (F ig. S7A). Concomitantly, the leaf weights were also smaller in the *C3H15*^{OE} plants and the shoot/root ratio was significantly higher in WT than in the *C3H15*^{OE} plants, indicating an enhanced development of roots in the *C3H15*^{OE} plants (Fi g. S7B).

The leaf chlorosis of *C3H15*^{OE} plants is accelerated in the four nutrient media used (Fig. 5, S8 and S9), although more intensely in the *C3H15*^{OE} plants grown under Cu deficiency. The variations of chlorophyll fluorescence in *C3H15*^{OE} and WT plants subjected to Cu and Zn deficiencies (Fig. 5B and S8B) Fv/Fm remained high during the first three weeks, at values typical of plants in good photosynthetic condition (0.80 ± 0.01, weeks 2 and 3). Subsequently, there was a strong decrease in the *C3H15*^{OE} plants, reaching statistical significance in plants grown in -Cu medium (F ig. S8B).

Importantly, in the case of the thickness of the floral scape, significant differences were observed among WT plants, specifically in Cu deficiency versus control (Fig. 5C). This result is consistent with a differential phenotypic effect on the floral stem because of forcing the overexpression of *C3H15* under Cu deficiency, a condition where its expression is inhibited in the WT plants.

Finally, the seed yield of plants grown in control medium averaged 0.48 g per plant in both genotypes (Table SIV). Growth in Cu or Zn deficient media increased seed production in the WT plants, similarly for both metals, while the effect was lower in Cu deficient the *C3H15*^{OE} plants. Taken together these data indicate that physiological and developmental processes are more intensely impaired in the *C3H15*^{OE} plants than in the WT plants regardless of the medium, and they are still more exacerbated under Cu deficient conditions further pointing to a long-distance problem in the Cu transport as a consequence of forcing *C3H15* expression.

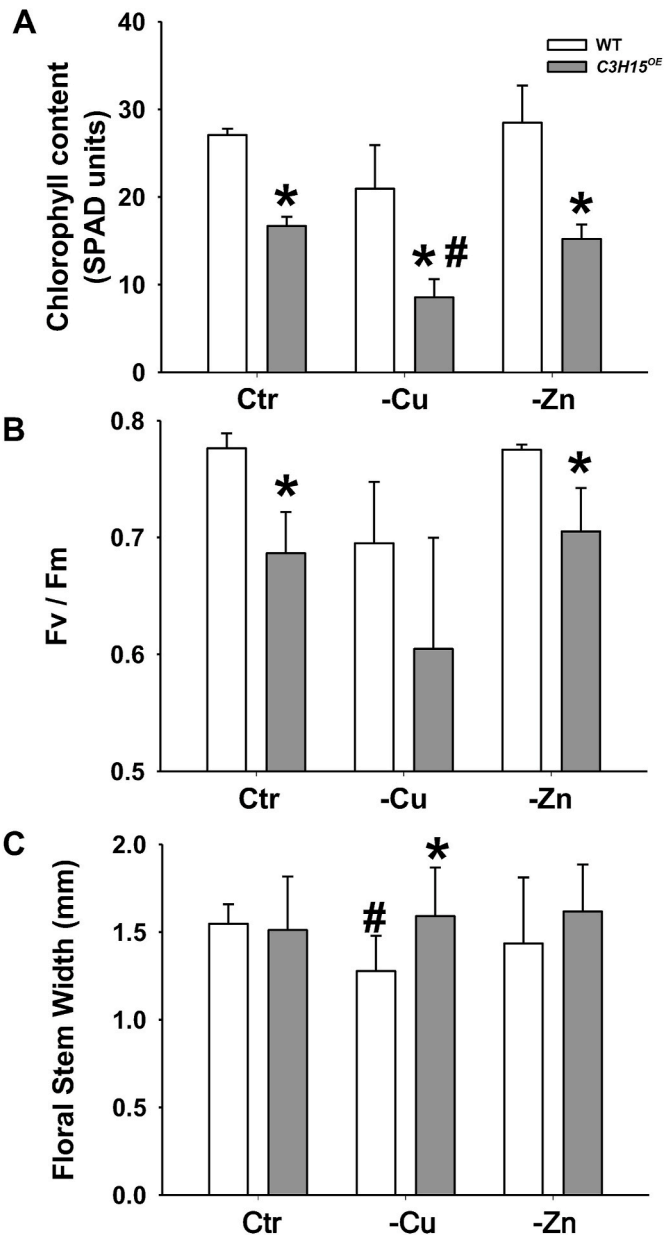

Fig. 5. Characterization of *C3H15*^{OE} hydroponic cultures. A) Chlorophyll content ±SD, and B) maximum quantum efficiency ±SD of PSII in dark-adapted state (Fv/Fm) of leaves of WT and *C3H15*^{OE} plants grown during four weeks in control conditions or in copper (-Cu) or zinc (-Zn) deficient medium. Three leaves per plant of four three-plant samples from two independent replicates were measured. C) Floral stem weight ±SD in the same conditions than A-B) from n = 8–9 samples. Statistical analysis was performed by one-way anova and subsequent Tukey'stest (A) or by Student t-tests (B) (n = 4, $p < 0.05$). * indicates significant differences between overexpressing and WT plants in the same condition # indicates significant differences between *C3H15*^{OE} under deficiency vs *C3H15*^{OE} under sufficiency conditions ($p < 0.05$).

3.8. Characterization of gene expression patterns at stems from plants with altered C3H15 levels grown under copper deficiency

Since the most severe phenotype was observed under Cu-deficient conditions in the reproductive organs, we analyzed the expression of the putative C3H15 targets previously described in the floral stems (Chai et al., 2015) and in Table I. According to a role of C3H15 as post-transcriptional negative regulator, the expression of *LHCB2.3*, *LAC17, SKS4* and *ENODL8* in *C3H15*^{OE} stems should be reduced

compared to the WT. It was unexpected that, this regulation was only observed under Cu deficiency (-Cu), but was oppositely increased under Cu sufficiency (Ctr) (Figure S10A). In order to evaluate the expression of C3H15 putative targets related to Cu homeostasis in floral stems, we analyzed in the same conditions the relative expression of the genes previously studied in seedlings: *SPL7, CCS, PETE2, ARPN, HMA5* and *COPT6* (Fig. 6). The general expression pattern was mostly similar to that observed for the previously described C3H15 targets. Thus, in general, gene expression was specifically down-regulated in the over-expressing plants under Cu deficiency conditions (except for *HMA5* and *COPT6* genes) whereas expression was increased in the *C3H15*^{OE} floral stems under control conditions. Once again, and as also shown for seedlings, the C3H15-mediated regulation of gene expression strongly depends on Cu availability, although these long-term effects are more difficult to assign as a direct effect of C3H15 on gene expression, and other indirect effects could also be taking place. In this sense, it is worth to mention that the general reduced expression is not observed in the Cu transporters *COPT6* and *HMA5* (Fig. 6), which maybe pointing to other superimposed regulatory effect due to an exacerbated Cu deficiency in the *C3H15*^{OE} floral stems. According to this, the expression of the Fe homeostasis genes such as *FSD1* and *FER3*, that have been shown to respond to Cu deficiency were exacerbated in the stems of the over-expressing plants under Cu deficiency, whereas *bHLH121* and *VTL2* expression showed a similar pattern to that already described for putative C3H15 targets (Figure S10B). Regarding Zn homeostasis, whereas gene expression of the corresponding putative targets was mostly increased under Cu sufficiency conditions in the *C3H15*^{OE} stems, this effect was not observed under Cu deficiency except for *ZAT12* (Figure S10C). Taken together, these data indicate a Cu-dependent effect of the regulatory role of the C3H15 protein on the expression of metal homeostasis genes with putative ARE motifs. However, the long-term and long-distance effects on the plant nutritional status preclude assigning a direct C3H15 role in the observed changes in gene expression.

3.9. Metal content by tissue in plants with altered C3H15 levels according to nutritional status

Since our final goal was to check if long-term effects of C3H15 overexpression affect long-distance nutrient redistribution in the plant, we analyzed the metal content by ICP-MS in different organs of WT and *C3H15*^{OE} adult plants grown in hydroponics media, under Cu sufficiency and deficiency (Fig. 7). As expected, under deficiency conditions Cu content was reduced in all the studied organs. However, seeds of the *C3H15*^{OE} are receiving a reduced Cu content under Cu deficiency. In the case of Fe content, no significant differences were observed between *C3H15*^{OE} and WT plants, with the exception of slightly higher levels in young leaves of the *C3H15*^{OE} (Fig. 7B). Regarding the Zn content, the *C3H15*^{OE} plants contain more Zn than the WT plants in the aerial part under Cu deficiency, although the Zn content in the seeds was also reduced (Fig. 7C).

Taken together, *C3H15*^{OE} plants seem to mobilize more metals to the aerial part under Cu-deficient conditions, although Cu and Zn fail to arrive to the seeds. This could indicate that despite an exacerbated metal relative distribution in the *C3H15*^{OE} plants, metal partition either outside/inside the cells and/or transport between cells through plasmodesmata is altered. It could be hypothesized that C3H15-dependent cell wall modifications are finally affecting metal retention and reducing the long-distance transport of Cu and Zn towards the seeds.

4. Discussion

In *S. cerevisiae*, the Cth1 and Cth2 proteins regulate gene expression under Fe deficiency at the post-transcriptional level by limiting mRNAs levels or inhibiting the translation of non-essential ferroproteins (Puig et al., 2005, 2008; Ramos-Alonso et al., 2018). However, it has not yet been explored whether the role of their counterparts in higher plants is related to metal homeostasis. Plant homologues are designated C3H14 and C3H15 or CDM1. The degree of divergence between these and their yeast counterparts could be compatible with an additional or different role. Specifically, the main divergence between yeast and plants can be observed in the CCCH2 motif and in the separation between the two CCCH motifs in Arabidopsis, which is further increased in ZmC3H14, OsC3H14 and OsC3H15 (Fig. 1A and S1A).

At the molecular level, TZF proteins bind to 3′-UTR regions of ARE-containing mRNAs through this domain. Our global analysis for the presence of AREs in the *Arabidopsis* genome indicates an over-representation of the category of metal homeostasis genes, including crucial relevant transcriptional regulators of Cu, Fe and Zn homeostasis (SPL7, bHLH21 and ZAT12, respectively). It is notable that, in contrast to yeast, the present study has failed to find any connection between Fe homeostasis and the role of Cth2 homologues in higher plants. However, the putative ARE–containing gene expression patterns in media with different Cu availability suggests that C3H15 may play a role as a negative post-transcriptional modulator on the expression of genes relevant to Cu homeostasis. Although, the transcriptional regulation of several of these ARE-containing Cu homeostasis factors is independent of the Cu content in the media, putative and still unknown and post-transcriptional regulatory mechanisms have been suggested to account for their specific function at different Cu levels. This is exemplified by SPL7, the major transcriptional regulator of Cu deficiency responses (Bernal et al., 2012; Yamasaki et al., 2009). As previously described, *SPL7* expression levels remain constant at different Cu concentrations in WT plants (Fig. 3B). The specific SPL7 function under Cu deficiency has been claimed to be the result of posttranscriptional and/or post-translational regulatory mechanisms. In this regard, it has been demonstrated that Cu^{2+} ions can substitute Zn at the SPL7 Zn finger domains, thereby interfering negatively with their DNA-binding capacity. This suggests the existence of a potential Cu sensing mechanism (Sommer et al., 2010). Moreover, a potential interaction between SPL7 and KIN17 proteins specific to certain tissues/organs has been suggested, responsive to fulfilling of distinct Cu uptake and distribution and demand (Garcia-Molina et al., 2014). Study presents evidence that *SPL7* transcript level could be affected by C3H15 through its putative ARE sequence, depending on the Cu content of the media (Table 1 and Figs. 3 and 6). This regulation could further extend its effects to the multiple of SPL7 targets, greatly affecting Cu deficiency responses.

Other genes with similar transcriptional rates under different Cu statuses and suspected to be post-transcriptionally modulated are *CCS* and *PETE2*. In the case of *PETE2*, a post-transcriptional mechanism has been proposed since the protein is known to be regulated via Cu accumulation (Abdel-Ghany, 2009). Like *SPL7*, *CCS* and *PETE2* transcripts present putative ARE elements and their regulation in *C3H15*^{OE} plants is compatible with the C3H15 function as a direct Cu-dependent modulator (Table 1 and Figs. 3 and 6). On the other hand, *ARPN* encodes a vacuole-localised multi-copper oxidase whose expression has been proposed to affect the metal availability in plastids for essential proteins such as plastocyanin or hormone biosynthetic enzymes (abscisic acid and gibberellins) (Jiang et al., 2021). The fact that C3H15 may act as a post-transcriptional negative modulator of all these genes depending on environmental Cu bioavailability points to the complex interplay affecting Cu homeostasis and the subsequent effects on plant development through hormonal changes, reduced photosynthesis and accelerated senescence (Fig. 5 and S6).

Cu partioning between the cell wall and the cytosol is an important factor in Cu homeostasis. Cell wall modifications affect metal binding and retention capacity affecting both cellular and whole-plant Cu redistribution via internal and long-distance Cu transport (Yruela, 2009). In addition, multiple multicopper oxidases, representing a high quota of cellular Cu, reside in the cell wall contributing to its properties (Perea-García et al., 2022). In this sense, the fact that putative cell wall-localised multicopper oxidases including LAC17, SKS4 and

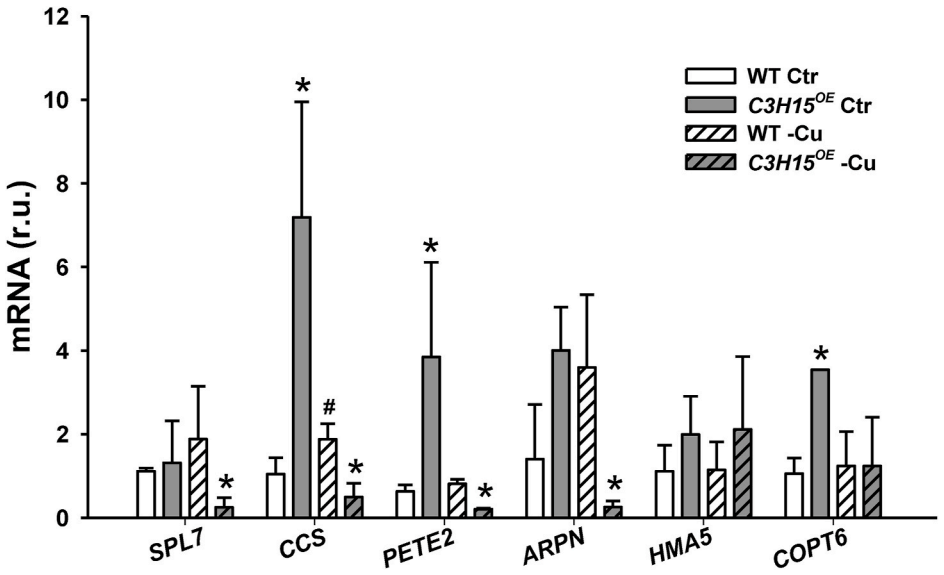

Fig. 6. Pattern expression in floral stems of copper homeostasis genes. The relative expression of the *SPL7*, *CCS*, *PETE2*, *ARPN*, *HMA5* and *COPT6* genes were determined by RT-qPCR in floral stems of WT and *C3H15*^{OE} plants, grown in different concentrations of Cu, deficiency (-Cu) and sufficiency (Ctr) in the medium. The *ACTIN2* and *UBQ10* genes were used as housekeeping genes. mRNA levels are expressed as relative units (r.u.). The bars represent the mean ± SD of three replicates. * indicates significantly differences between overexpressing plants against its WT in the same condition, # indicates significantly differences of WT vs WT under sufficiency condition ($p < 0.05$).

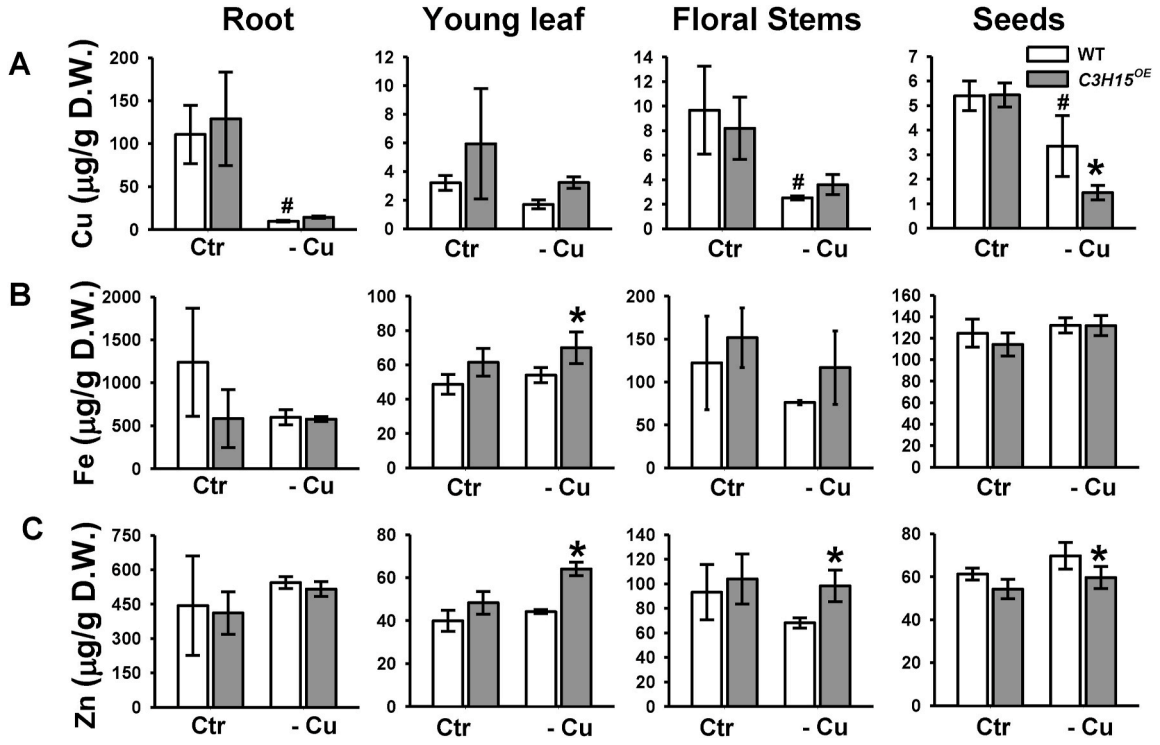

Fig. 7. Metal content in different tissue of hydroponic plants. Metal content (Cu, Fe and Zn) in roots, young leaves, floral stems and seeds of WT and *C3H15*^{OE} plants grown in control (Ctr) conditions or in copper (-Cu) or zinc (-Zn) deficiency medium for the last four weeks of growth. The bars represent the mean ± SD of three replicates. Statistical analysis was performed by two-way anova Duncan's test. * indicates significant differences between overexpressing plants against its WT in the same condition, # indicates significant differences of WT vs WT under sufficiency condition ($p < 0.05$).

ENODL8 are also regulated by C3H15 points to modulation of their levels as a key process in the adaptation of Cu homeostasis under non-optimal Cu supply (Table 1, F igs. S4 and S10). High Cu levels have been shown to be toxic specially in roots, blocking tip growth (Lequeux et al., 2010). Cu detoxification strategies may include increased root-to-shoot translocation when plants are subjected to Cu excess (Andrés-Colás et al., 2006). Based on our results, C3H14/C3H15 could take part of the remobilisation/translocation process for root Cu detoxification. However, once in the aerial part, although Cu is necessary for development, specially in the reproductive organs, Cu excess could also be toxic. In this regard, the mechanisms that prevent cell-to-cell transport through plasmodesmata have been shown to be

affected by Cu levels, which modulate their permeability through callose synthesis and degradation (O'Lexy et al., 2018).

Despite displaying similar Cu levels in floral stems, *C3H15*^{OE} plants show symptoms compatible with perceiving exacerbated Cu deficiency. Even under control conditions, *C3H15*^{OE} plants overexpressed several of the Cu deficiency markers, including *CCS, COPT6, ZIP4* and *NAS1* (Fig. 6 and S10). However, under Cu deficiency at least part of the response is abolished, maybe due to the down-regulation of the master regulator SPL7 transcription factor in the *C3H15*^{OE} plants. It is noteworthy that a part of the Cu deficiency response is maintained under Cu escarcity in the *C3H15*^{OE} plants. This is exemplified by the increased expression of *FSD1* and *miR398,* which are widely recognised Cu deficiency markers for Cu/ZnSOD substitution (F igs. S10 and S11) (Yamasaki et al., 2007). In addition, the expression of the gene encoding the P-type ATPase *HMA5* implicated in root-to-shoot Cu translocation (Andrés-Colás et al., 2006; Kobayashi et al., 2008), the expression of the Cu plasma membrane transporter *COPT6* (Garcia-Molina et al., 2013; Gayomba et al., 2013) and another Cu^{2+} transporter *ZIP4* are not repressed under Cu deficiency (Fig. 6 and S10). However, the strong reduction observed in the expression of the majority of genes encoding cuproproteins in *C3H15*^{OE} floral stems under Cu deficiency (Fig. 6) could be due to the fact of prolonged lack of Cu and, thereby further points to an exacerbated Cu deficiency perception in these plants. A more conclusive data reinforcing this are the reduced Cu levels in *C3H15*^{OE} seeds when the plants are grown under low Cu conditions (Fig. 7). Thus, the *C3H15*^{OE} phenotypes observed under Cu deficiency respond to the forced high *C3H15* expression under conditions where its expression would otherwise remain low. These phenotypes may be due to the complex interplay of the C3H15 functions in both previously shown cell wall remodelling and metal homeostasis, as shown here. These functions could also affect the mobilisation of other ions, such as Zn and Fe, as indicated in this work (Figs. 4 and 7). Although *C3H15*^{OE} plants mobilize metals towards the aerial part under Cu-deficient conditions, Cu and Zn fail to arrive to the seeds and we did not observe changes on the seeds Fe content (Fig. 7). This fact could indicate that despite an exacerbated metal relative distribution in *C3H15*^{OE} plants, metal partitioning either outside/inside the cells and/or transport between cells through plasmodesmata is altered. In the case of Fe, a different strategy for Fe detoxification or to compensatory effects in Fe homeostasis regulation could be behind the lack of differences in seed Fe content. In any case, our data on *C3H15*^{OE} discard a role of plants Cth2 homologues similar to the previously described function on Fe deficiency modulation in yeast (Puig et al., 2005).

This work suggests that metal homeostasis and cell wall remodelling are mutually interacting processes intricately connected through the *C3H15* function. In this sense, ARE-containing metal homeostasis genes as putative C3H15 targets would probably serve to modulate or compensate the metal translocation changes derived from C3H15-dependent cell wall remodelling that occurs in different tissues and developmental stages with the aim of adapting and optimizing plant growth to non-optimal metal conditions in the medium. This work uncovers the function of the C3H15 protein as a putative link between the modulation of metal homeostasis and the previously cell wall composition through a common posttranscriptional regulatory mechanism. Although complex to address, knowledge of these processes is necessary to consider future biotechnological applications to regulate the metal content in crops grown in soils with non-optimal metal supplies, thereby preventingtoxic metals from reaching edible organs.

5. Conclusions

This study identifies C3H15 as a post-transcriptional regulator involved in the Arabidopsis homeostasis of copper and zinc, despite C3H15 being the closest yeast Cth2 homologue, which participates in iron adaptation under deficiency. The previously described role of C3H15 in cell wall modification could also affect metal translocation as suggested by accelerated senescence occurring in plants with deregulated levels of C3H15 grown under Cu deficiency conditions. Moreover, these overexpressing C3H15 plants show a lower metal content in seeds. Taken together these results point to an intertwined role between cell wall modification and metal transport processes and indicate the importance of its comprehension for future biotechnological applications in plants of agronomic interest.

Authors contribution

Sergi Puig, Amparo Sanz and Lola Peñarrrubia conceived the project; Amparo Andrés-Bordería, Antoni Garcia-Molina, Nuria Andrés-Colás, Laia Mazuque-Pons, Marta Romeu-Perales and Amparo Sanz performed the experiments. María Teresa Martinez-Pastor analyzed the *in silico* data. Lola Peñarrubia and Ana Perea-Garcia designed the experiments and wrote the manuscript. All authors contributed to review the article and approved the submitted version.

Declaration of competing interest

The authors declare that they have no known competing financial interests or personal relationships that could have appeared to influence the work reported in this paper.

Data availability

The institutional open access repository of the Spanish National Research Council DIGITAL.CSIC

Acknowledgements

We acknowledge Dr Patricia Casino for her help with the overlapping of the TZF domains, Dr Zhou for the C3H14, C3H15 overexpressing seeds and *c3h14c3h15(±)* mutant and Marta Olmos for her technical support. A. Sanz obtained a sabbatical year grant (UV-PDI_SAB-156039). We acknowledge the SCSIE (Universitat de València) for the ICP-MS service. This research was funded by the Spanish Ministry of Economy and Competitiveness "PID2020-116940RB-I00 and PID2023-148124OB-I00 funded by MCIN/AEI/10.13039/501100011033" and CIGE/2021/092 funded by Generalitat Valenciana.

Appendix A. Supplementary data

Supplementary data to this article can be found online at https://doi.org/10.1016/j.plaphy.2024.109123.

References

Abdel-Ghany, S.E., 2009. Contribution of plastocyanin isoforms to photosynthesis and copper homeostasis in *Arabidopsis thaliana* grown at different copper regimes. Planta 229, 767–779. https://doi.org/10.1007/s00425-008-0869-z.

Abdel-Ghany, S.E., Müller-Moulé, P., Niyogi, K.K., Pilon, M., Shikanai, T., 2005. Two P-type ATPases are required for copper delivery in *Arabidopsis thaliana* chloroplasts. Plant Cell 17, 1233–1251. https://doi.org/10.1105/tpc.104.030452.

Abdel-Ghany, S.E., Pilon, M., 2008. MicroRNA-mediated systemic down-regulation of copper protein expression in response to low copper availability in Arabidopsis. J. Biol. Chem. 283, 15932–15945. https://doi.org/10.1074/jbc.M801406200.

Ahn, Y., Jun, Y., 2007. Measurement of pain-like response to various NICU stimulants for high-risk infants. Early Hum. Dev. 83, 255–262. https://doi.org/10.1016/j.earlhumdev.2006.05.022.

Andrés-Colás, N., Perea-García, A., Mayo De Andrés, S., Garcia-Molina, A., Dorcey, E., Rodríguez-Navarro, S., Pérez-Amador, M.A., Puig, S., Peñarrubia, L., 2013. Comparison of global responses to mild deficiency and excess copper levels in Arabidopsis seedlings. Metallomics 5, 1234–1246. https://doi.org/10.1039/c3mt00025g.

Andrés-Colás, N., Perea-García, A., Puig, S., Peñarrubia, L., 2010. Deregulated copper transport affects Arabidopsis development especially in the absence of environmental cycles. Plant Physiol. 153, 170–184. https://doi.org/10.1104/pp.110.153676.

Andrés-Colás, N., Sancenón, V., Rodríguez-Navarro, S., Mayo, S., Thiele, D.J., Ecker, J.R., Puig, S., Peñarrubia, L., 2006. The Arabidopsis heavy metal P-type ATPase HMA5

interacts with metallochaperones and functions in copper detoxification of roots. Plant J. 45, 225–236. https://doi.org/10.1111/j.1365-313X.2005.02601.x.
Balandin, T., Castresana, C., 2002. AtCOX17, an Arabidopsis homolog of the yeast copper chaperone COX17. Plant Physiol. 129, 1852–1857. https://doi.org/10.1104/pp.010963.
Bernal, M., Casero, D., Singh, V., Wilson, G.T., Grande, A., Yang, H., Dodani, S.C., Pellegrini, M., Huijser, P., Connolly, E.L., Merchant, S.S., Krämer, U., 2012. Transcriptome sequencing identifies SPL7-regulated copper acquisition genes FRO4/FRO5 and the copper dependence of iron homeostasis in Arabidopsis. Plant Cell 24, 738–761. https://doi.org/10.1105/tpc.111.090431.
Bogamuwa, S.P., Jang, J.C., 2014. Tandem CCCH zinc finger proteins in plant growth, development and stress response. Plant Cell Physiol. 55, 1367–1375. https://doi.org/10.1093/pcp/pcu074.
Burkhead, J.L., Gogolin Reynolds, K.A., Abdel-Ghany, S.E., Cohu, C.M., Pilon, M., 2009. Copper homeostasis. New Phytol. 182, 799–816. https://doi.org/10.1111/j.1469-8137.2009.02846.x.
Chai, G., Kong, Y., Zhu, M., Yu, L., Qi, G., Tang, X., Wang, Z., Cao, Y., Yu, C., Zhou, G., 2015. Arabidopsis C3H14 and C3H15 have overlapping roles in the regulation of secondary wall thickening and anther development. J. Exp. Bot. 66, 2595–2609. https://doi.org/10.1093/jxb/erv060.
Chai, G., Liu, H., Zhang, Y., Wang, C., Xu, H., He, G., Meng, J., Tang, X., Wang, D., Zhou, G., 2024. Integration of C3H15-mediated transcriptional and post-transcriptional regulation confers plant thermotolerance in Arabidopsis. Plant J. 1–12. https://doi.org/10.1111/tpj.16877.
Curie, C., Mari, S., 2017. New routes for plant iron mining. New Phytol. 214, 521–525. https://doi.org/10.1111/nph.14364.
Dong, J., Kim, S.T., Lord, E.M., 2005. Plantacyanin plays a role in reproduction in Arabidopsis. Plant Physiol. 138, 778–789. https://doi.org/10.1104/pp.105.063388.
Easlon, H.M., Bloom, A.J., 2014. Easy Leaf Area: automated digital image analysis for rapid and accurate measurement of leaf area. Appl. Plant Sci. 2 https://doi.org/10.3732/apps.1400033.
Garcia-Molina, A., Andrés-Colás, N., Perea-García, A., Neumann, U., Dodani, S.C., Huijser, P., Peñarrubia, L., Puig, S., 2013. The Arabidopsis COPT6 transport protein functions in copper distribution under copper-deficient conditions. Plant Cell Physiol. 54, 1378–1390. https://doi.org/10.1093/pcp/pct088.
Garcia-Molina, A., Xing, S., Huijser, P., 2014. A conserved KIN17 curved DNA-binding domain protein assembles with SQUAMOSA PROMOTER-BINDING PROTEIN-LIKE7 to adapt Arabidopsis growth and development to limiting copper availability. Plant Physiol. 164, 828–840. https://doi.org/10.1104/pp.113.228239.
Gayomba, S.R., Jung, H. Il, Yan, J., Danku, J., Rutzke, M.A., Bernal, M., Krämer, U., Kochian, L.V., Salt, D.E., Vatamaniuk, O.K., 2013. The CTR/COPT-dependent copper uptake and SPL7-dependent copper deficiency responses are required for basal cadmium tolerance in *A. thaliana*. Metallomics 5, 1262–1275. https://doi.org/10.1039/c3mt00111c.
He, S.L., Li, B., Zahurancik, W.J., Arthur, H.C., Sidharthan, V., Gopalan, V., Wang, L., Jang, J.C., 2024. Overexpression of stress granule protein TZF1 enhances salt stress tolerance by targeting ACA11 mRNA for degradation in Arabidopsis. Front. Plant Sci. 15, 1–18. https://doi.org/10.3389/fpls.2024.1375478.
Hermans, C., Verbruggen, N., 2005. Physiological characterization of Mg deficiency in *Arabidopsis thaliana*. J. Exp. Bot. 56, 2153–2161. https://doi.org/10.1093/jxb/eri215.
Jang, J.C., 2016. Arginine-rich motif-tandem CCCH zinc finger proteins in plant stress responses and post-transcriptional regulation of gene expression. Plant Sci. https://doi.org/10.1016/j.plantsci.2016.06.014.
Jiang, A., Guo, Z., Pan, J., Yang, Y., Zhuang, Y., Zuo, D., Hao, C., Gao, Z., Xin, P., Chu, J., Zhong, S., Li, L., 2021. The PIF1-miR408-PLANTACYANIN repression cascade regulates light-dependent seed germination. Plant Cell 33, 1506–1529. https://doi.org/10.1093/plcell/koab060.
Kim, W.C., Ko, J.H., Han, K.H., 2012. Identification of a cis-acting regulatory motif recognized by MYB46, a master transcriptional regulator of secondary wall biosynthesis. Plant Mol. Biol. 78, 489–501. https://doi.org/10.1007/s11103-012-9880-7.
Kim, S.A., LaCroix, I.S., Gerber, S.A., Guerinot, M. Lou, 2019. The iron deficiency response in *Arabidopsis thaliana* requires the phosphorylated transcription factor URI. Proc. Natl. Acad. Sci. U.S.A. 116, 24933–24942. https://doi.org/10.1073/pnas.1916892116.
Kobayashi, Y., Kuroda, K., Kimura, K., Southron-Francis, J.L., Furuzawa, A., Kimura, K., Iuchi, S., Kobayashi, M., Taylor, G.J., Koyama, H., 2008. Amino acid polymorphisms in strictly conserved domains of a P-type ATPase HMA5 are involved in the mechanism of copper tolerance variation in Arabidopsis. Plant Physiol 148, 969–980. https://doi.org/10.1104/pp.108.119933.
Lai, W.S., Perera, L., Hicks, S.N., Blackshear, P.J., 2014. Mutational and structural analysis of the tandem zinc finger domain of tristetraprolin. J. Biol. Chem. 289, 565–580. https://doi.org/10.1074/jbc.M113.466326.
Lequeux, H., Hermans, C., Lutts, S., Verbruggen, N., 2010. Response to copper excess in Arabidopsis thaliana: Impact on the root system architecture, hormone distribution, lignin accumulation and mineral profile. Plant Physiol. Biochem. 48, 673–682. https://doi.org/10.1016/j.plaphy.2010.05.005.
Li, Z., Thomas, T.L., 1998. PEI1, an embryo-specific zinc finger protein gene required for heart-stage embryo formation in Arabidopsis. Plant Cell 10, 383–398. https://doi.org/10.1105/tpc.10.3.383.
Lu, P., Chai, M., Yang, J., Ning, G., Wang, G., Ma, H., 2014. The Arabidopsis CALLOSE DEFECTIVE MICROSPORE1 gene is required for male fertility through regulating callose metabolism during microsporogenesis. Plant Physiol. 164, 1893–1904. https://doi.org/10.1104/pp.113.233387.
Nagae, M., Nakata, M., Takahashi, Y., 2008. Identification of negative cis-acting elements in response to copper in the chloroplastic iron superoxide dismutase gene of the moss *Barbula unguiculata*. Plant Physiol. 146, 1687–1696. https://doi.org/10.1104/pp.107.114868.
O'Lexy, R., Kasai, K., Clark, N., Fujiwara, T., Sozzani, R., Gallagher, K.L., 2018. Exposure to heavy metal stress triggers changes in plasmodesmatal permeability via deposition and breakdown of callose. J. Exp. Bot. 69, 3715–3728. https://doi.org/10.1093/jxb/ery171.
Perea-García, A., Garcia-Molina, A., Andrés-Colás, N., Vera-Sirera, F., Pérez-Amador, M. A., Puig, S., Peñarrubia, L., 2013. Arabidopsis copper transport protein COPT2 participates in the cross talk between iron deficiency responses and low-phosphate signaling. Plant Physiol. 162, 180–194. https://doi.org/10.1104/pp.112.212407.
Perea-García, A., Puig, S., Peñarrubia, L., 2022. The role of post-transcriptional modulators of metalloproteins in response to metal deficiencies. J. Exp. Bot. 73, 1735–1750. https://doi.org/10.1093/jxb/erab521.
Pfaffl, M.W., Horgan, G.W., Dempfle, L., 2002. Relative expression software tool (REST) for group-wise comparison and statistical analysis of relative expression results in real-time PCR. Nucleic Acids Res. 30, e36. https://doi.org/10.1093/nar/30.9.e36 e36.
Pilon, M., Cohu, C.M., Ravet, K., Abdel-Ghany, S.E., Gaymard, F., 2009. Essential transition metal homeostasis in plants. Curr. Opin. Plant Biol. 12, 347–357. https://doi.org/10.1016/j.pbi.2009.04.011.
Pomeranz, M., Lin, P.C., Finer, J., Jang, J.C., 2010. AtTZF gene family localizes to cytoplasmic foci. Plant Signal. Behav. 5, 190–192. https://doi.org/10.4161/psb.5.2.10988.
Puig, S., Askeland, E., Thiele, D.J., 2005. Coordinated remodeling of cellular metabolism during iron deficiency through targeted mRNA degradation. Cell 120, 99–110. https://doi.org/10.1016/j.cell.2004.11.032.
Puig, S., Vergara, S.V., Thiele, D.J., 2008. Cooperation of two mRNA-binding proteins drives metabolic adaptation to iron deficiency. Cell Metabol. 7, 555–564. https://doi.org/10.1016/j.cmet.2008.04.010.
Ramos-Alonso, L., Romero, A.M., Soler, M.À., Perea-García, A., Alepuz, P., Puig, S., Martínez-Pastor, M.T., 2018. Yeast Cth2 protein represses the translation of ARE-containing mRNAs in response to iron deficiency. PLoS Genet. 14 https://doi.org/10.1371/journal.pgen.1007476.
Sanvisens, N., Romero, A.M., An, X., Zhang, C., de Llanos, R., Martínez-Pastor, M.T., Bañó, M.C., Huang, M., Puig, S., 2014. Yeast Dun1 kinase regulates ribonucleotide reductase inhibitor Sml1 in response to iron deficiency. Mol. Cell Biol. 34, 3259–3271. https://doi.org/10.1128/mcb.00472-14.
Sommer, F., Kropat, J., Malasarn, D., Grossoehme, N.E., Chen, X., Giedroc, D.P., Merchant, S.S., 2010. The CRR1 nutritional copper sensor in Chlamydomonas contains two distinct metal-responsive domains. Plant Cell 22, 4098–4113. https://doi.org/10.1105/tpc.110.080069.
Sun, J., Jiang, H., Xu, Y., Li, H., Wu, X., Xie, Q., Li, C., 2007. The CCCH-type zinc finger proteins AtSZF1 and AtSZF2 regulate salt stress responses in Arabidopsis. Plant Cell Physiol. 48, 1148–1158. https://doi.org/10.1093/pcp/pcm088.
Wang, D., Guo, Y., Wu, C., Yang, G., Li, Y., Zheng, C., 2008. Genome-wide analysis of CCCH zinc finger family in Arabidopsis and rice. BMC Genom. 9, 1–20. https://doi.org/10.1186/1471-2164-9-44.
Wang, Y., Yang, J., Miao, R., Kang, Y., Qi, Z., 2021. A novel zinc transporter essential for Arabidopsis zinc and iron-dependent growth. J. Plant Physiol. 256 https://doi.org/10.1016/j.jplph.2020.153296.
Waters, B.M., McInturf, S.A., Stein, R.J., 2012. Rosette iron deficiency transcript and microRNA profiling reveals links between copper and iron homeostasis in *Arabidopsis thaliana*. J. Exp. Bot. 63, 5903–5918. https://doi.org/10.1093/jxb/ers239.
Xie, M., Sun, J., Gong, D., Kong, Y., 2019. The roles of arabidopsis C1-2i subclass of C2H2-type zinc-finger transcription factors. Genes 10. https://doi.org/10.3390/genes10090653.
Yamasaki, H., Abdel-Ghany, S.E., Cohu, C.M., Kobayashi, Y., Shikanai, T., Pilon, M., 2007. Regulation of copper homeostasis by micro-RNA in Arabidopsis. J. Biol. Chem. 282, 16369–16378. https://doi.org/10.1074/jbc.M700138200.
Yamasaki, H., Hayashi, M., Fukazawa, M., Kobayashi, Y., Shikanai, T., 2009. SQUAMOSA promoter binding protein-like7 is a central regulator for copper homeostasis in Arabidopsis. Plant Cell 21, 347–361. https://doi.org/10.1105/tpc.108.060137.
Yruela, I., 2009. Copper in plants: acquisition, transport and interactions. Funct. Plant Biol. 36, 409–430. https://doi.org/10.1071/FP08288.
Zhang, Y., Xu, Y.H., Yi, H.Y., Gong, J.M., 2012. Vacuolar membrane transporters OsVIT1 and OsVIT2 modulate iron translocation between flag leaves and seeds in rice. Plant J. 72, 400–410. https://doi.org/10.1111/j.1365-313X.2012.05088.x.